Free-growth properties of a nematic–smectic-B liquid-crystal interface

Ágnes Buka and Tibor Tóth Katona
Research Institute for Solid State Physics of the Hungarian Academy of Sciences, H-1525 Budapest, P.O.B. 49, Hungary

Lorenz Kramer
Institute of Physics, University of Bayreuth, D-95440 Bayreuth, Germany
(Received 8 June 1994)

Three types of smectic-B (Sm-B) germs with respect to the director orientation inside and outside the germ have been found. Two of them are planar and one is homeotropic. The equilibrium shapes have been recorded and the angle dependence of the surface tension has been determined by Wulff construction. The planar germs undergo a dramatic change of morphology as a function of undercooling, starting from an elongated, rectanglelike shape to dendritic growth of fourfold symmetry. Near equilibrium the homeotropic germs have a circular form with a small hexagonal modulation, and show a dense branching morphology for larger undercoolings. Growth rates have been measured and compared for all types of germs in a wide range of undercooling.

PACS number(s): 61.30.−v, 61.50.Cj, 64.70.Md

I. INTRODUCTION

Nonequilibrium crystal growth resulting in complex pattern morphologies such as dendrites or dense branching have been intensively studied theoretically [1–6]. There are several precise experimental studies on pure substances that form dendrites during the phase transition. Measurements on ice, metals, succinonitrile, cyclohexanol, krypton, etc., are known [7–10].

Dendritic growth of *liquid-crystal* phases has also been observed for a certain range of supersaturation in columnar structures constructed of disklike molecules [11, 12]. One-component, thermotropic liquid crystals of rodlike molecules show rarely complex patterns by their phase transitions. Dendrites of a smectic-B–smectic-A interface were observed in a directional solidification experiment [13]. Free growth of dendritic and dense branching smectic germs nucleating in the nematic (N) phase have been reported in [14, 15]. A more complete investigation using several materials will be presented here.

II. EXPERIMENT

Three liquid-crystalline substances were used for the experiments, each of them having a nematic to smectic-B first-order phase transition at T_{NS}, temperatures given in parenthesis denote monotropic transitions,

(I) 4-n-propyl-4′-cyano-trans 1,1-bicyclohexane, T_{NS} = (56.3 °C),

(II) 4-n-butyl-N-[4-(p-cyanophenyl)-benzylidene]-aniline, T_{NS} = (87.4 °C),

(III) 4-n-propyl-4′-trifluoromethoxyphenyl-ethylene-trans 1,1-bicyclohexane, T_{NS} = 77.0 °C.

Sandwich cells of dimensions 10 mm×10 mm×10 μm were prepared between two parallel glass plates. Samples of both surface alignments of the nematic director—homeotropic and planar— were studied, with an exception of substance III for which no homeotropic orientation could be obtained.

For planar alignment of the nematic director we used commercial liquid-crystal cells KSRP-10 with polyamid coating and rubbing, manufactured by E.H.C. Co., Ltd. from Japan. The inner surfaces of the cells, under the polyamid layers, are also coated with thin conductive layers that serve as electrodes in case of measurements in the electric field. For making cells with a homeotropically aligned nematic phase, glass plates of 1-mm thickness with SnO_2 coating have been used. In order to assure the homeotropic orientation, a layer of octadecyl-triethoxy-silane was transferred onto the inner surfaces by polymerization.

The sample temperature was controlled in a hot stage with an accuracy of 0.002 °C. Other details of the experimental setup have been given elsewhere [16].

III. RESULTS

Three types of smectic-B germs (Fig. 1) in equilibrium with the nematic phase have been found in a quasi-two-dimensional geometry [16]. Two of these [Fig. 1(a) and 1(b)] have a similar, rectanglelike shape with two long, faceted sides parallel with the smectic layers and with slightly convex boundaries on the short sides. Both germs are planar (P), the smectic director—indicated with double arrows — lies in the plane of the picture, parallel to the glass plates. The difference is that the surrounding nematic is planar in Fig. 1(a) and homeotropic (H) in Fig. 1(b). Thus the director orientation is the same on both sides of the interface in case of Fig. 1(a)—P(in P)—and changes by an angle of 90° in Fig. 1(b)—P(in H). In the last case one has an additional contribution to the surface energy coming from the elastic deformation of the nematic phase near the interface which is of splay-bend type along the long edges and mainly twist along

the short ones. This deformation zone has a width on the order of the sample thickness d and is barely visible in Fig. 1(b). In thicker samples one can see a set of clear interference fringes.

The smectic-B phase nucleates in the nematic fluid, away from the glass plates (in the interior of the sample) which is a favorable condition for creating perfect smectic ordering. The director of the smectic body is presumably parallel with that of the nematic phase until its linear size (diameter) approaches the sample thickness. During further growth the germ usually prefers an orientation where its director is parallel with the glass surfaces (smectic layers are perpendicular to them). This configuration is naturally fulfilled for planar initial alignment of the nematic phase resulting in the P(in P) geometry. In the homeotropic samples most germs turn by an angle of $\pi/2$ before reaching the glass plates and keep growing in the P(in H) configuration.

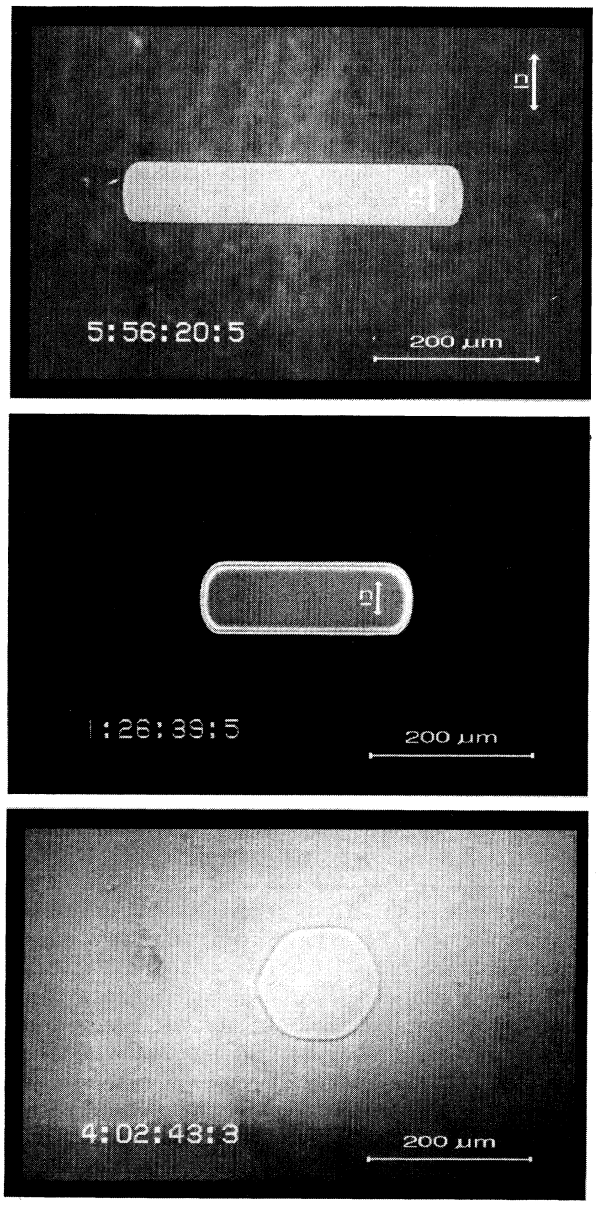

FIG. 1. Microscopic images of equilibrium shapes of Sm-B germs in contact with the nematic phase, $d = 10$ μm (substance I). In order to obtain the age of the Sm-B monodomains 10 h have to be added to the counting given in the pictures. Double arrows indicate direction of director, (a) planar Sm-B in planar N; P(in P), (b) planar Sm-B in homeotropic N; P(in H), (c) homeotropic Sm-B in homeotropic N; H(in H).

The third type of the equilibrium Sm-B germs is homeotropic (the smectic director is perpendicular to the plane of the picture) and has a circular shape with a small hexagonal modulation [Fig. 1(c)]. It was observed in a homeotropic nematic surrounding—H(in H)—thus there is no change of the director across the pattern boundary. The H(in H) configuration can spontaneously be seen very rarely because the germs in the homeotropic cells usually turn over spontaneously to be planar and form the P(in H) configuration. We tried to influence the orientation of the smectic body imbedded in the nematic phase by applying an electric field perpendicular to the glass plates. The substances have strong positive dielectric anisotropy resulting in parallel orientation of the director and the electric field which corresponds to the homeotropic alignment. Nevertheless, the germs turned over to be planar up to a field of 50 V/10 μm.

By melting a planar germ until it again gets so small that it turns back to homeotropic orientation and then applying a fast cooling before the germ melts and disappears completely, a homeotropic germ can be obtained. Due to the large undercooling the homeotropic germ grows rapidly without having the chance to turn back again.

The shape anisotropy of the equilibrium germs is reflected in the anisotropy of the surface tension function $\sigma(\theta)$, which can be obtained from the equilibrium shape by the Wulff construction [17]. This was carried out for a planar germ in [16] (θ is the angle of the surface normal). In Fig. 2 the surface tension is plotted for the three cases given in Fig. 1. We only show a relevant angle segment and we have included simple fit formulas that reflect the symmetries and may be useful for comparison with other experimental or theoretical results. Further segments can be obtained by continuing σ symmetrically and periodically. For the H(in H) configuration we have averaged the shape function over the 12 symmetry-equivalent segments to obtain better accuracy. Note that for the two planar germs one has to continue symmetrically also beyond $\theta = \pi/2$ so that one here has a cusp that is associated with the faceting of these germs along their long sides. As a measure of the anisotropy we use the quantity $\varepsilon = (\sigma_{max} - \sigma_{min})/(\sigma_{max} + \sigma_{min})$, which actually coincides with the shape anisotropy $(R_{max} - R_{min})/(R_{max} + R_{min})$ where the radius R measures the distance of the germ perimeter from its nucleation point [18, 19]. ε is very large for the planar germs: 0.49 and 0.68 for the P(in H) and P(in P) respectively. For the P(in H) germ the surface tension actually has a very shallow minimum at $\theta = 0$, see [16], which exludes a polynomial fit with few terms. To circumvent this difficulty the vicinity of $\theta = 0$ was left out in the fit [see Fig. 2(b)]. For the homeotropic

H(in H) germ with weak hexagonal symmetry $\varepsilon = 0.03$ and this value is essentially equal with the amplitude of the basic Fourier mode $\cos(6\theta)$.

Concerning the dynamics, e.g., growth of the Sm-B phase at different values of undercooling ($\Delta T = T_{NS} - T$), several morphologies of growth patterns have been observed. First, we describe the qualitative features of the growth forms, which are very different for the planar and homeotropic Sm-B germs while the alignment of the nematic surrounding does not seem to influence the morphology. Some results on the growth for the P(in H) geometry for substance II have previously been published [15]. The shape of planar, single smectic germs even for large undercoolings is similar in the two geometries P(in P) and P(in H), the only difference appears in the orientation of single seeds, which is random in the homeotropic nematic [no anisotropy in the plane of the pattern, see Fig. 3(b)] and uniform in the planar nematic [Fig. 3(a)]. In the last case the main branches of the Sm-B dendrites make an angle of 45° with the nematic director.

Growth of the Sm-B phase was observed at and below T_{NS} with smectic seeds formed *spontaneously* in the process of cooling and with single grains prepared by heating spontaneous ones up to T_{NS}, i.e., *preserved seeds.*

In the case of *spontaneous nucleation* only the fast, dendritic growth of planar germs, as shown in Fig. 3, could be observed (because at small undercooling no spontaneous nucleation occurred on the time scale of hours) for substances I and III. A stable growth of the dendrite tip was then found with a well-defined velocity for each undercooling. Growth rates were determined by measuring the tip coordinates versus time, which was found to be a linear function with an accuracy of better than 1%. Velocities as a function of undercooling are given in Fig. 4 for the P(in P) configuration.

Substance II showed a high nucleation activity even for low undercooling but the observed growth velocity was not constant in the investigated range of $\Delta T = (0.6 - 2.3)\,^{\circ}\mathrm{C}$, it decreased with time as $v \sim t^{-\alpha}$ where α is about 0.9 for the P(in P). The same value for α was found earlier for the P(in H) geometry as published in [15].

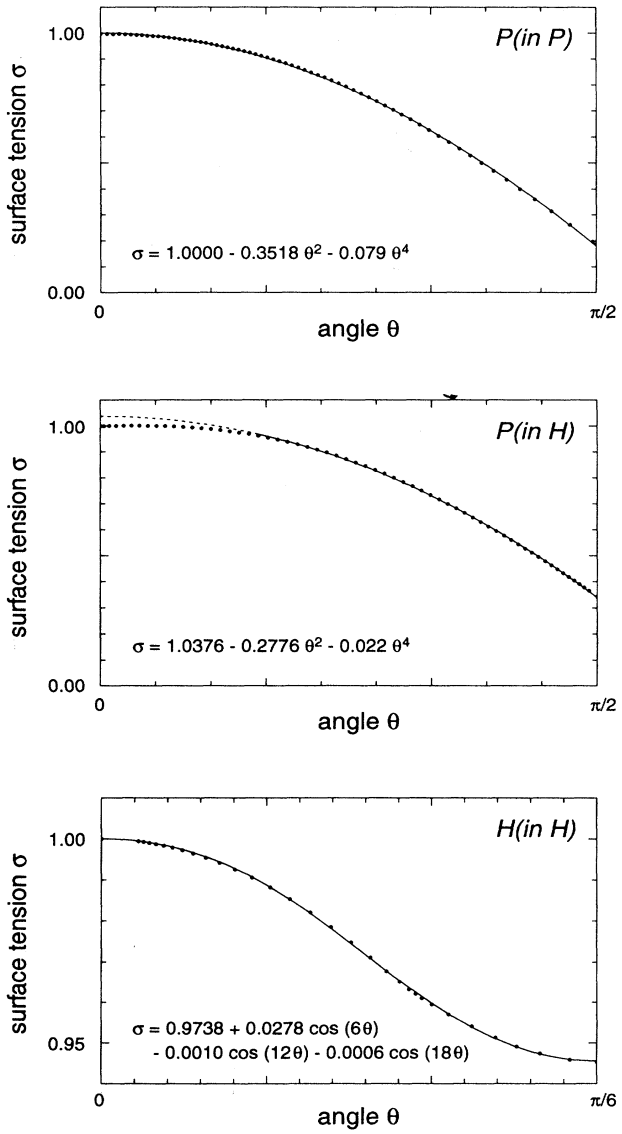

FIG. 2. Normalized surface tension $\sigma(\theta)$ as a function of the surface orientation (in rad) calculated from the equilibrium shapes shown in Figs. 1(a)–1(c).

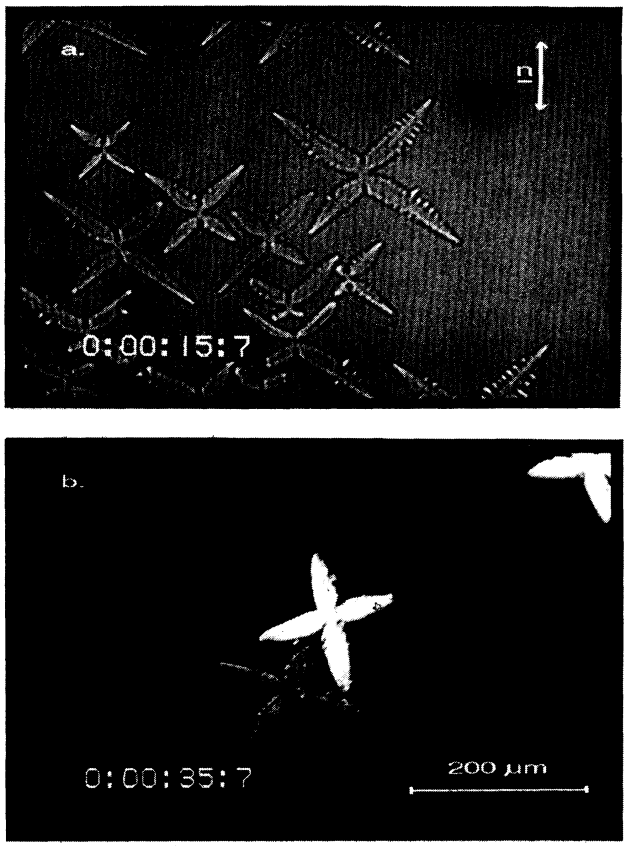

FIG. 3. Microscopic images of planar dendrites growing with a high velocity at $\Delta T = 0.5\,^{\circ}\mathrm{C}$ (a) P(in P), (b) P(in H).

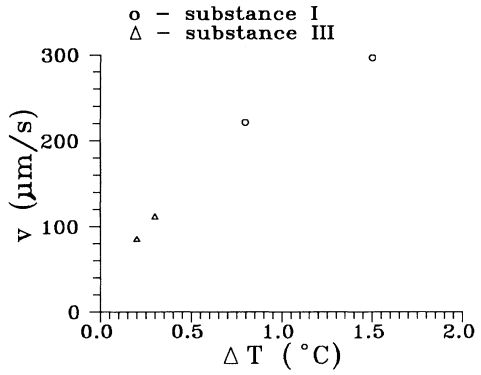

FIG. 4. Growth velocity of spontaneously formed planar germs at different undercoolings.

As already mentioned, H(in H) germs had to be prepared by manipulation of a preserved seed, thus no spontaneous growth could be studied. In experiments with a *preserved seed*, substance II showed qualitatively the same behavior as for spontaneous nucleation: growth velocity decreased with time with a similar exponent α.

For precise quantitative measurements we preferred to use the same germ that was kept unmelted during several cooling and heating cycles. Results shown in the following sections will be presented with such preserved seeds in all three configurations P(in P), P(in H), and H(in H) of substance I.

A. Morphology

The qualitative features of the planar and homeotropic germs are summarized as follows.

1. Planar germs: P(in P) and P(in H)

Figure 5 demonstrates the growth of planar Sm-B germs by showing plots of contours of the N–Sm-B boundary recorded at subsequent moments and copied on top of each other. The values of ΔT for Figs. 5(a)–5(d) are given in the figure caption together with the time passed since the thermal field was switched on.

The smectic germs are optically homogeneous. We detected total extinction of the light if the crossed polars pointed along the bisectrices of the main branches of the growing pattern thus along x and y in Fig. 5. Using a quartz wedge we determined the optical axis (director) of the smectic germs which is parallel to y while (x, z) is the plane of the smectic layers. Thus faceted sides in Figs. 5(a) and 5(b) are parallel with the smectic layers. The director of the surrounding nematic is either parallel to y which is the P(in P) configuration, or lies along z leading to P(in H).

As a function of undercooling the following morphologies have been observed:

(a) The *equilibrium morphology*, i.e., the rectanglelike shape with convex short sides, persists in a small range of undercooling just below T_{NS} and a slow dynamics is observed in this *quasiequilibrium regime* [see Fig. 5(a)].

(b) In the next range of ΔT the short sides become *concave* forming the four main branches, which grow parallel with the smectic layers in this regime, while the long sides stay faceted [Fig. 5(b)].

(c) This shape is called *butterfly*, faceting vanishes in this regime and the branches open up. The shape of the tips remains asymmetric with respect to its growth direction (nonparabolic tip growth), see Fig. 5(c).

(d) At large undercooling one gets typical *dendritic* growth (parabolic tips), with the four main branches at an average angle of 90° with some variation from germ to germ [Fig. 5(d)]. This morphology is rather puzzling, because there is no fourfold symmetry in the system.

2. Homeotropic germ: H(in H)

Figure 6 shows the growth of the homeotropic Sm-B germ demonstrated in a similar way as the planar ones in Fig. 5. Smectic and nematic directors are perpendicular to the plane of the picture which corresponds also to the plane of the smectic layers. The seed is circular at the beginning and above a certain radius a hexagonal modulation develops. We divide the observed patterns into two morphologies:

(a) The *equilibrium morphology* persists in a small

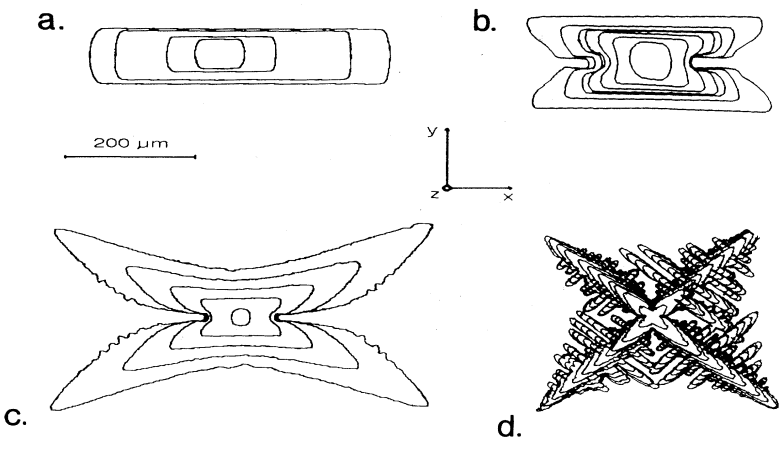

FIG. 5. Different morphologies of planar smectic germs (substance I, also in all following figures). The growth is demonstrated by plotting the contours of the images taken at subsequent times on top of each other. (a) equilibrium shape, $\Delta T = 0.08\,^{\circ}$C, t =11.7 s; 1 min 23.7 s; 6 min 54.7 s; 10 min 8.1 s, (b) concave shape, $\Delta T = 0.1\,^{\circ}$C, t = 0.2 s; 8.4 s; 12.4 s; 16.7 s; 21.6 s; 26.9 s; 31.4 s, (c) butterfly, $\Delta T = 0.3\,^{\circ}$C, t =0.6 s; 3.3 s; 5.7 s; 7.5 s; 10.1 s, (d) dendrite, $\Delta T = 0.5\,^{\circ}$C, t =0.1 s; 1.1 s; 1.6 s; 2.1 s; 2.8 s; 3.3 s; 3.9 s; 4.2 s 4.6 s; 5.1 s; 5.6 s.

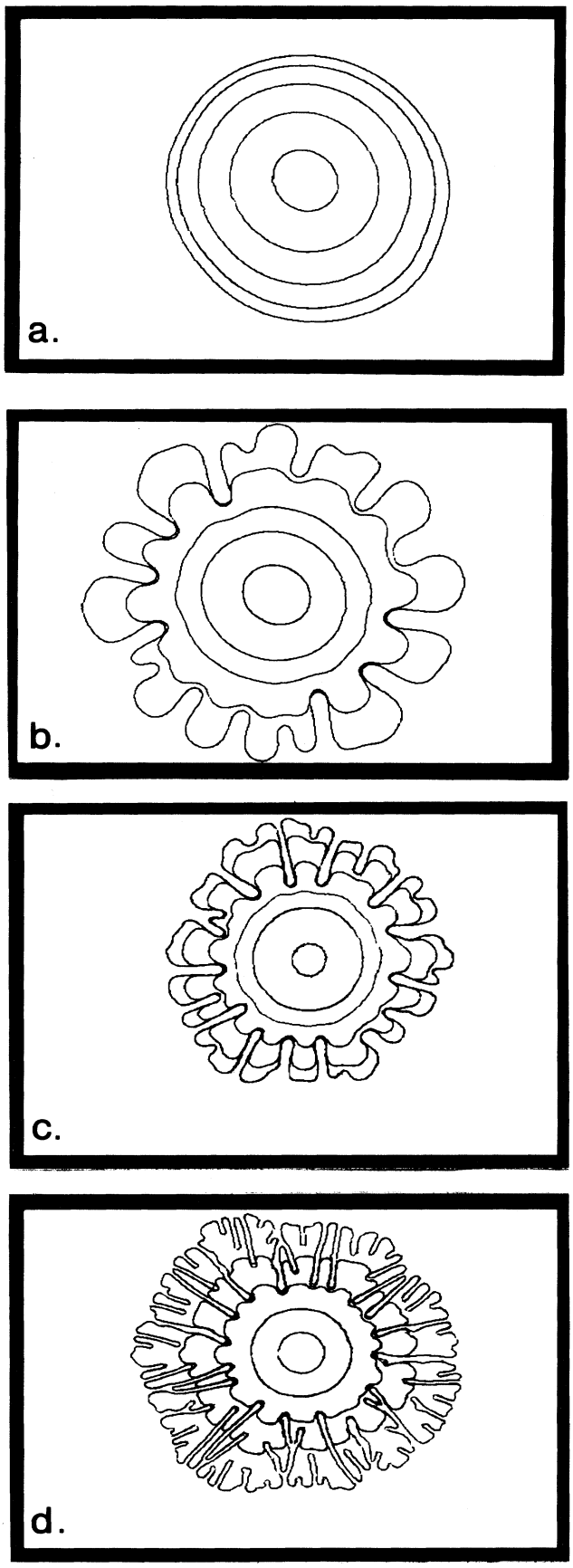

range of undercooling see Fig. 6(a). (Though after reaching an area of the order of 10^5 $(\mu m)^2$ the form of the germ will be irregular—"puddle shaped".)

(b) For larger ΔT a *dense-branching* regime was observed which persists in the whole experimentally realizable range, see Figs. 6(b)–(d). The pattern is highly space filling (dense) and its enveloping curve preserves the hexagonal shape.

The qualitative features of the H(in H) germ is very similar to that of a columnar phase driven by supersaturation [12]. There also, a dendritic growth is observed for intermediate undercooling between the equilibrium morphology and the dense branching.

B. Growth dynamics

In this section we give a quantitative description of the growth properties of the N–Sm-B interface. Because the tip velocity is ambiguous for nondendritic morphologies, see e.g., Figs. 5(a) and 5(b), we measure the area A of the patterns and plot the square root of it versus time or undercooling. In this way we can compare the growth dynamics of patterns for any shape or morphology. We determined for a P(in P) dendrite in substance II the time evolution of the tip velocity and that of $d\sqrt{A}/dt$. Both velocities vary like $\sim t^{-\alpha}$ with the same α.

Because the growth behavior has a strong dependence on ΔT we define three regimes: *slow, intermediate* and *fast.* In Fig. 7 the *slow* regime is demonstrated which extends up to about $\Delta T = 0.1°$ and corresponds to the *equilibrium morphology* for all three types of germs: P(in P), P(in H), and H(in H). In fact, there are small shape changes during the growth of planar germs, namely an increase of the length to width ratio (compared to that in equilibrium) and a slight straightening of the convex short sides. When ΔT is decreased to achieve slow shrinkage the shape changes will be reversed.

The growth velocity decreases with time in this regime for all three germs. Comparing Figs. 7(a), 7(b), and 7(c) one can say that the growth of P(in H) is the fastest followed by P(in P) and H(in H). We repeat that this regime can only be studied with already existing germs (at such small undercooling no spontaneous nucleation occurs).

A peculiar effect was observed for very small undercoolings. The growth rate decreased continuously, reached zero (the growth stopped), and went on with increasing negative values till the germ disappeared. A detailed quantitative study of this effect is in progress.

Figure 8 demonstrates the *intermediate* regime where after a transient effect the growth occurs with a con-

FIG. 6. Different morphologies of homeotropic seeds. The scale is the same as in Fig. 5 (a). Quasiequilibrium shape, $\Delta T = 0.05\,°C$, $t = 0.5$ s; 3 min 42.5 s; 8 min 22.2 s; 13 min 40.0 s; 18 min 0.3 s; (b) dense branching, $\Delta T = 0.15\,°C$, t =0.5 s; 58.3 s; 1 min 21.2 s; 1 min 58 s; 2 min 32.2 s; (c) dense branching, $\Delta T = 0.4\,°C$, t =0.6 s; 24.8 s; 30.9 s; 37.4 s; 42 s; 44.5 s; (d) dense branching, $\Delta T = 0.9\,°C$, t =0.5 s; 8.8 s; 14.1 s; 17.3 s; 20.4 s.

stant velocity. These growth rates are given in the figure (for substance I). For comparison we also give the velocity for substance III in the P(in P) configuration: $v = (6.6 \pm 0.1)$ μm/s, for $\Delta T = 0.1\,^{\circ}$C. Morphologically it is the regime where planar germs get concave on the short sides [see Fig. 5(b)] and homeotropic ones start forming fingers [Fig. 6(b)] (i.e., equilibrium is replaced

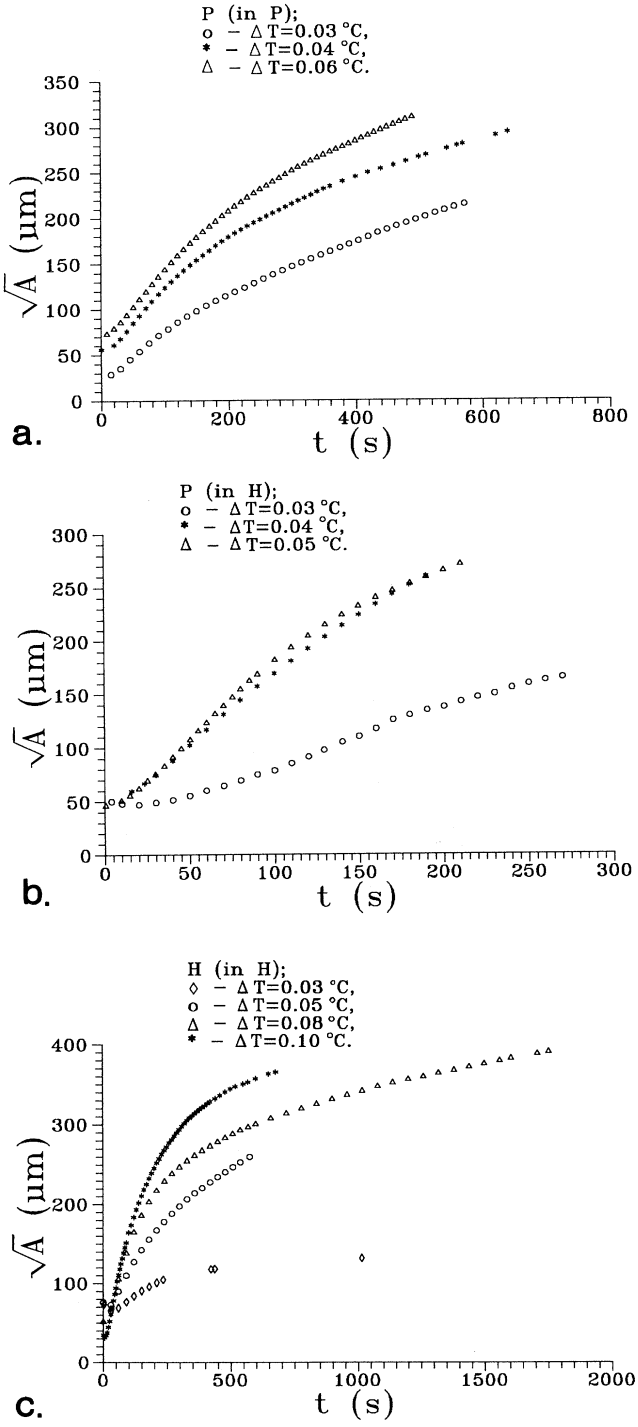

FIG. 7. Square root of the germ area versus time in the slow regime.

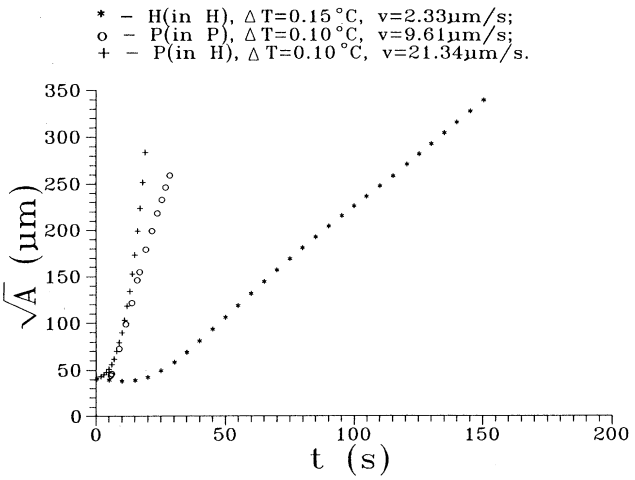

FIG. 8. Growth dynamics for intermediate range. Square root of the area versus time. Velocities given in the picture correspond to the slope of the linear part of the curves.

by nonequilibrium growth). Presumably in both cases the growth process has undergone an instability. The transient presumably involves thermal relaxation of the cell which is dominated by the heat diffusing through the cell boundaries made of $l = 1$ mm thick glass. With a heat diffusivity of $D = 10^{-2}$ cm^2 s^{-1} one obtains for the typical time $\tau = l^2/D \approx 1$ s which is consistent with the measurements.

We mention here a technical limitation of our recording system, namely we can follow the growth up to a linear size of about 500 μm, consequently for fast processes we cannot record the growth for long times.

The *fast* regime that occurs for $\Delta T > 0.2\,^{\circ}$C and corresponds to dendritic growth for the planar and to dense branching for the homeotropic germs is demonstrated in Fig. 9. The velocity increases with time for all types of germs (an overall acceleration) which we believe to be a transient possibly followed by a linear regime. P(in H) remains the fastest for these undercoolings too, followed by the P(in P), showing that dendritic growth is more rapid than that of the dense branching morphology in H(in H).

It is very surprising that the Sm-B germ grows faster in the P(in H) configuration than in the P(in P) (with the similar morphology), in spite of the presence of the deformation in the P(in H) (the smectic director turns over by an angle of 90° during the process of the phase transition).

IV. DISCUSSION AND CONCLUSION

In the quasiequilibrium regime the dynamics can be understood by diffusive slowing down of a compact interface, see [1]. This leads to $v \sim t^{-\alpha}$ with $\alpha = 1/2$. Experimental values for α were found in the range of 0.7 ± 0.2. Figure 10 shows examples of time dependences of the growth velocities $v = d\sqrt{A}/dt$ for each configuration—P(in P), P(in H), and H(in H)—obtained from the data of Figs. 7(a), 7(b), and 7(c). The curves represent the

fit to $v \sim t^{-\alpha}$. The values obtained for α with the experimental errors are shown in the figure. The error is somewhat larger than in the case of spontaneous nucleation. For substance III in the P(in P) configuration the parameter α has practically the same value (0.67 ± 0.01) as for substance I.

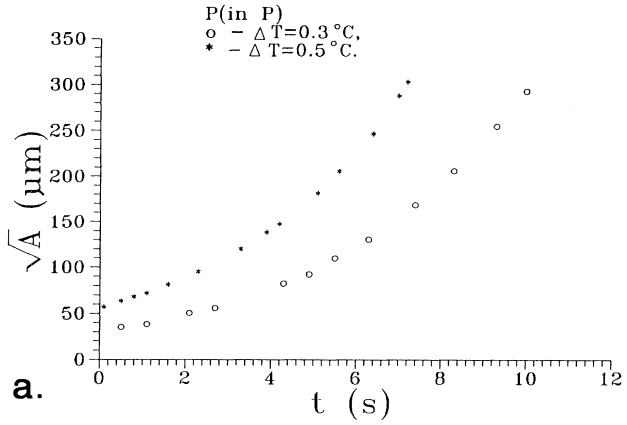

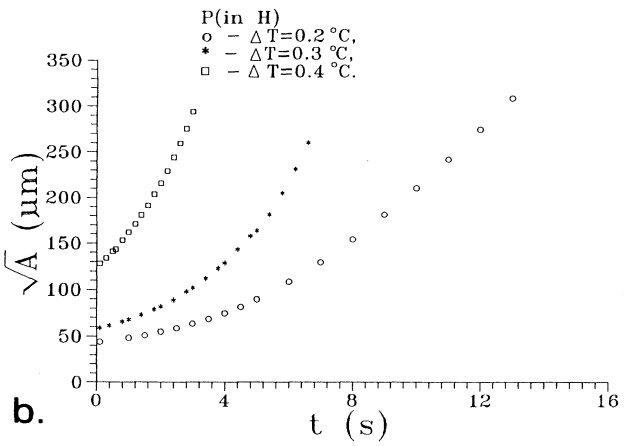

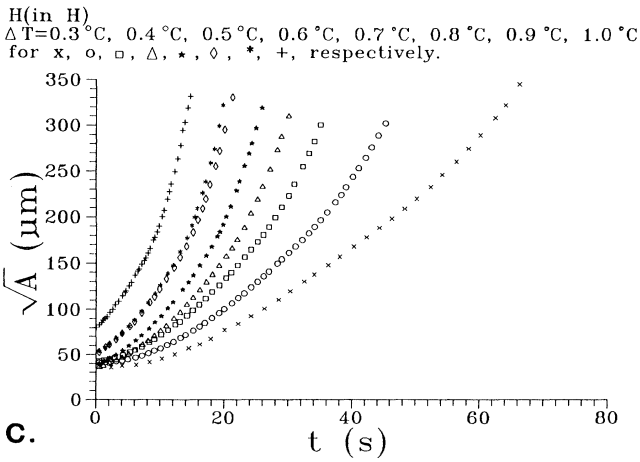

FIG. 9. Growth dynamics in the fast regime. Time dependence of the square root of the germ area for (a) P(in P), (b) P(in H), and (c) H(in H).

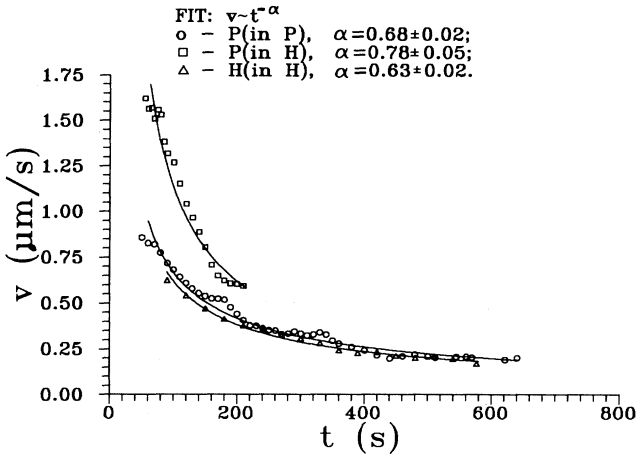

FIG. 10. Growth velocities versus time in the slow regime. The undercoolings are $\Delta T = 0.05\,^{\circ}\mathrm{C}$ for P(in H) and H(in H) and $\Delta T = 0.04\,^{\circ}\mathrm{C}$ for P(in P). The fitted curves are described in the text.

The transition to more complex morphologies at larger undercoolings is accompanied by the growth velocity tending to be asymptotically constant. This is a generic feature of growth phenomena after the equilibrium morphology has become unstable [3, 4]. The case of H(in H) is rather conventional in the sense that the anisotropy (of the surface tension) is small. One then expects at first dendritic growth and at larger undercooling, when the influence of anisotropy becomes insignificant, tip-splitting growth leading to dense branching morphology. In our case the dendritic growth regime could be expected between $\Delta = 0.005$ and $\Delta = 0.015$ [see Figs. 6(a) and 6(b)], where Δ is the dimensionless undercooling [20]. This range was not studied experimentally carefully enough for substance I. Dendritic growth in the above range of undercooling was observed in a similar nematic material not discussed here [21]. We point out that in the experiments on columnar phases dendritic growth was observed up to about $\Delta = 0.5$ though the anisotropy there was smaller by about one order of magnitude [11, 12].

An interesting observation is that the hexagonal modulation of the equilibrium shape [Fig. 1(c)] and that of the envelope at large undercooling [Fig. 6(d)] have the same phase (the relative orientation of the direction of maxima coincide). This is not trivial because in one case the effect is caused by the surface tension anisotropy and in the other it originates from the anisotropy of kinetic effects. A shift of 30° between the orientation of maxima was found for a columnar hexagonal phase [22].

In the case of planar germs the anisotropy is large and, therefore, tip splitting is not observed. The first instability leads to concaving of the short sides, which can presumably be interpreted as a Mullin-Sekerka-type instability of the fastest growing portion of the interface [Fig. 5(b)]. The next step is a kinetic roughening of the faceted sides starting from the tip region. Actually for substance II we observed a destabilization of the faceted sides, too, before the roughening. This leads to intrusions in the central portions, see [15]. In the final den-

dritic regime the anisotropy appears to have only a local effect (e.g., stabilization of the tips) whereas the global morphology is ruled solely by the repulsive interaction of the tips. Otherwise the (apparent) fourfold symmetry observed in all three materials could not be understood.

It would seem desirable to substantiate the above qualitative remarks by quantitative theoretical studies with models that have the appropriate (large) anisotropy built in and take into account the quasi-two-dimensional geometry of the sample heated from the plates. The parametrizations of the angle-dependent surface tensions given in Fig. 2 are useful in this context, in fact, promising preliminary computations based on a phase field model with surface tension anisotropy [24] reproduce qualitatively several experimentally observed morphologies [23]. Surface tension anisotropy without faceting has also been incorporated in another type of phase field model [25].

ACKNOWLEDGMENTS

Substance II was synthesized by K. Fodor-Csorba; materials I and III were kindly made available for us by Merck, Darmstadt. We wish to thank R. Kupferman for valuable discussions. The work was financially supported by the Hungarian Academy of Sciences Grant No. OTKA 2976 and the Volkswagen Foundation. A.B. wishes to thank the University of Bayreuth for its hospitality and the Alexander von Humboldt Foundation for the equipment donation.

[1] J.S. Langer, Rev. Mod. Phys. **52**, 1 (1980); in *Chance and Matter*, edited by J. Souletie, J. Vannimenus, and R. Stora, Les Houches, Session XLVI (Plenum, New York, 1987), Chap. 10.

[2] D. Kessler, J. Kopik, and H. Levine, Adv. Phys. **37**, 255 (1988).

[3] E. Ben-Jacob and P. Garik, Nature **343**, 523 (1990).

[4] E. Brener, H. Mueller-Krumbhaar, and D. Temkin, Europhys. Lett. **17**, 535 (1992).

[5] O. Shochet, K. Kassner, E. Ben-Jacob, S.G. Lipson, and H. Mueller-Krumbhaar, Physica **181**, 136 (1992); **187**, 87 (1992).

[6] Y. Tu, H. Levine, and D. Ridgeway, Phys. Rev. Lett. **71**, 3838 (1993).

[7] K. Koo, R. Ananth, and W.N. Gill, Phys. Rev. A **44**, 3782 (1991).

[8] D.E. Ovsienko, G.A. Alfintsev, and V.V. Maslov, J. Cryst. Growth **26**, 233 (1974).

[9] S.C. Huang and M.E. Glicksman, Acta Metall. **29**, 701 (1981); **29**, 717 (1981).

[10] J.H. Bilgram, M. Firmann, and E. Huerlimann, J. Cryst. Growth **96**, 175 (1989).

[11] P. Oswald, J. Phys. (Paris) **49**, 1083 (1988).

[12] P. Oswald, J. Malthete, and P. Pelce, J. Phys. **50**, 2121 (1989).

[13] J. Bechhoefer, P. Oswald, A. Libchaber, and C. Germain, Phys. Rev. A **37**, 1691 (1988).

[14] S. Arora, A. Buka, P. Palffy-Muhoray, Z. Racz, and R. Vora, Europhys. Lett. **7**, 43 (1988).

[15] A. Buka and N. Eber, Europhys. Lett. **21** (4), 477 (1993).

[16] A. Buka, T. Toth Katona, and L. Kramer, Phys. Rev. E **49**, 5271 (1994).

[17] See, e.g., M. Wortis, in *Fundamental Problems in Statistical Mechanics VI*, Proceedings of the 1984 Trondheim Summer School, edited by E.G.D. Cohen (North Holland, Amsterdam, 1985), p. 87; H. van Beijeren and I. Nolden, in *Structure and Dynamics of Surfaces II*, edited by W. Schommers and P. van Blankenhagen (Springer-Verlag, Berlin, 1987), p. 259.

[18] A. Dougherty, J. Cryst. Growth **110**, 501 (1991).

[19] M. Muschol, D. Liu, and H.Z. Cummins, Phys. Rev. A **46** (2), 1038 (1992).

[20] The dimensionless undercooling is $\Delta = \Delta T c_p/L \approx \Delta T/(13\ \mathrm{K})$ for substance I.

[21] A. Buka, T. Toth Katona, and T. Börzsönyi (unpublished).

[22] J.C. Geminard, P. Oswald, D. Temkin, and J. Malthete, Europhys. Lett. **22** (1), 69 (1993).

[23] A. Hernandez-Machado, R. Gonzalez-Cinca, L. Ramirez-Piscina, and J. Casademunt (private communication).

[24] G.B. McFadden, A.A. Wheeler, R.J. Braun, and S.R. Coriell, Phys. Rev. E **48**, 2016 (1993).

[25] R. Kupferman, O. Shochet, and E. Ben-Jacob, Phys. Rev. E **50**, 1005 (1994).

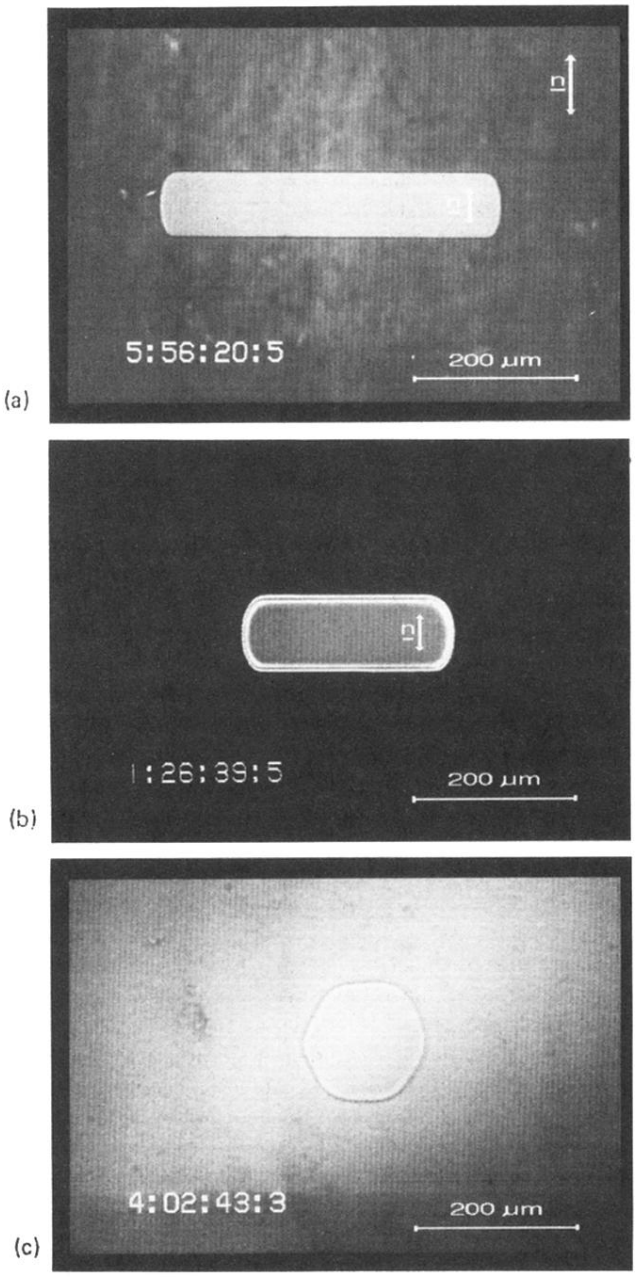

FIG. 1. Microscopic images of equilibrium shapes of Sm-B germs in contact with the nematic phase, $d = 10$ μm (substance I). In order to obtain the age of the Sm-B monodomains 10 h have to be added to the counting given in the pictures. Double arrows indicate direction of director, (a) planar Sm-B in planar N; P(in P), (b) planar Sm-B in homeotropic N; P(in H), (c) homeotropic Sm-B in homeotropic N; H(in H).

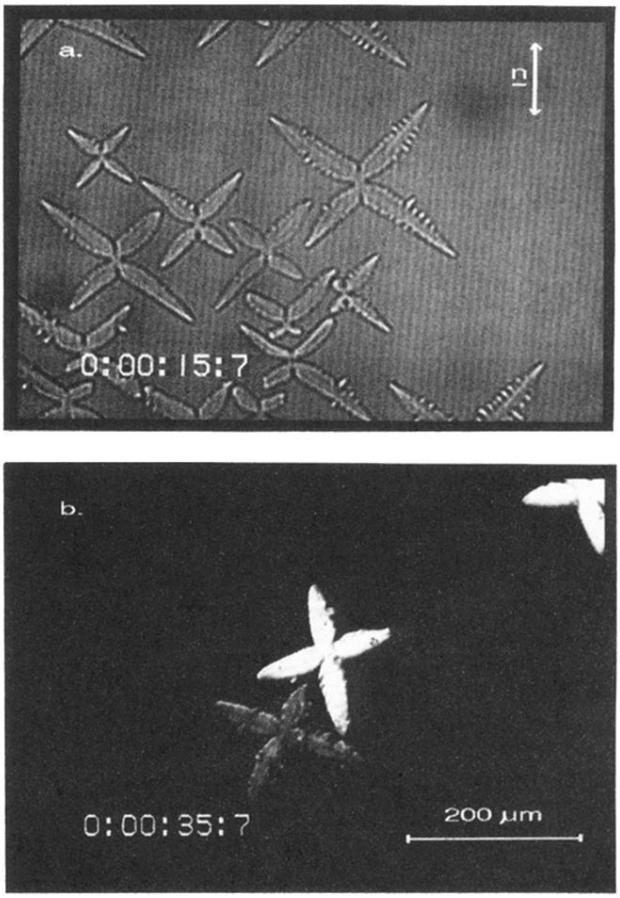

FIG. 3. Microscopic images of planar dendrites growing with a high velocity at $\Delta T = 0.5\,^{\circ}\mathrm{C}$ (a) P(in P), (b) P(in H).